Bulletin of the Seismological Society of America, Vol. 85, No. 1, pp. 83–92, February 1995

Liquefaction during the 1990 Manjil, Iran, Earthquake, II: Case History Analyses

by M. K. Yegian, V. G. Ghahraman, M. A. A. Nogole-Sadat, and H. Daraie

Abstract Liquefaction and liquefaction-induced permanent ground deformations and building settlements were widespread during the 1990 Manjil, Iran, earthquake (M_S = 7.7). In the first of these companion articles, geologic, seismologic, and geotechnical data of liquefaction case histories were presented. This article presents results of the analysis of (1) the ground-motion data; (2) liquefaction strength corresponding to level ground conditions; (3) permanent lateral ground deformations; (4) residual shear strength of the liquefied sands; and (5) settlement of buildings on liquefied sands.

Introduction

In the companion article (Yegian *et al.*, 1995), the authors describe the results of field surveys and investigations of liquefaction and liquefaction-induced damage from the 1990, Manjil, Iran, earthquake. Case histories are identified that relate to liquefaction of level ground, permanent ground deformation, and liquefaction-induced settlement of buildings. To document the relevant geotechnical data for these case histories, geotechnical field investigations were performed using the standard penetration test (SPT) equipment. The modified SPT, $(N_1)_{60}$ values, the blow counts corrected for the effect of overburden pressure and energy ratio (Seed *et al.*, 1983), and the grain-size distribution of the liquefied and nonliquefied sands were obtained at 33 locations throughout the liquefied region. The companion article presents the borehole logs of these case histories together with the general description of the geology of the liquefied region. It also includes a complete list of peak ground acceleration values obtained from this earthquake.

This article presents analyses of the recorded ground motion and of the geotechnical data from the Manjil earthquake. Case histories corresponding to liquefaction of level ground are analyzed following the empirical procedure described by Seed *et al.* (1983). The strength against liquefaction, as determined by analysis of the case history data, is compared with that given by Seed *et al.* (1983). In addition, analysis of permanent lateral ground deformations is made to evaluate the residual (minimum) shear strength of the liquefied sands. Finally, the measured field settlement values of level ground and of buildings on liquefied sands are analyzed and the results are compared with those obtained by other theoretical and empirical procedures.

Ground Motions

The ground motions during the Manjil earthquake were recorded at 15 stations. Figure 1 shows a plot of peak accelerations of the two horizontal components of the recorded ground motions versus the distance of the recording stations from the fault. Also in Figure 1, a comparison is made between the recorded data and the attenuation relationships proposed by Idriss (1990) and Joyner and Boore (1988). It is noted that, in general, the Manjil data match well with the attenuation relationship of Idriss (1990). Hence, for case histories located between 10 and 50 km from the fault, where recorded data are lacking, ground accelerations were estimated from this relationship. However, for the case histories located near the Caspian Sea, 60 to 85 km from the fault, the ground surface accelerations were obtained based on the record at Lahijan located 62 km from the ruptured fault.

The recording station closest to city of Astaneh-Ashrafieh was at Lahijan, 20 km southeast of Astaneh-Ashrafieh. The soil profile at these two cities is generally characterized as 50 to 70 m of alluvium overlying bedrock (Nogole-Sadat, 1992). Thus, in the analyses of liquefaction case histories in the Astaneh-Ashrafieh region, the recorded ground motion from Lahijan was used.

Figure 2 shows the transverse component of the acceleration time history recorded in Lahijan (Naderzadeh, 1991, personal comm.). Although the trace of the digitized record shows a total duration of 60 sec, the duration of interest for liquefaction analysis is considerably shorter. To illustrate this, the equivalent number of uniform cycles, N_{eq}, of the Lahijan record was computed as a function of time using the procedure suggested by Seed *et al.* (1975). Figure 3 shows the result, which indicates that the record has a total of about 17 equivalent uniform cycles and an "effective" duration of about 15 sec. This calculated value of N_{eq} = 17 cycles from an earthquake

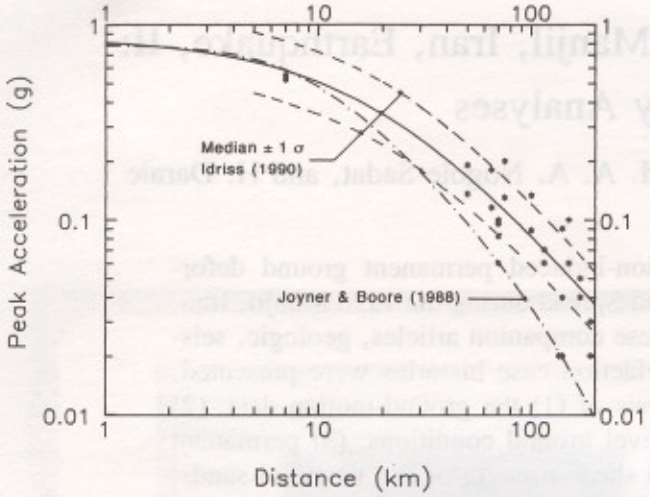

Figure 1. Recorded peak ground accelerations versus distance to the fault breakout from the 1990 Manjil, Iran, earthquake.

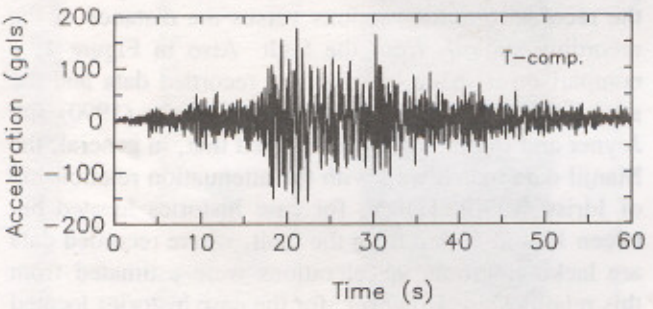

Figure 2. Recorded acceleration time history, in the transverse direction, in Lahijan, during the 1990 Manjil, Iran, earthquake (Naderzadeh, 1991, personal comm.).

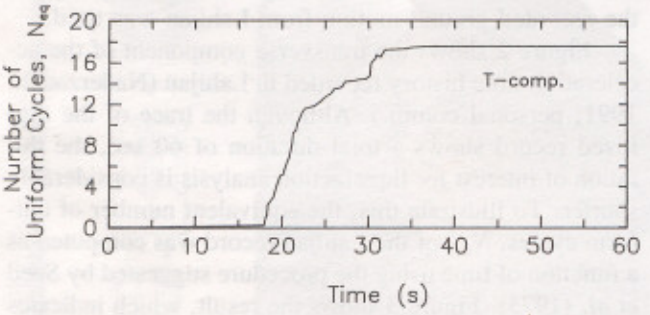

Figure 3. Equivalent number of uniform cycles of the recorded ground motion calculated from the Lahijan record shown in Figure 2.

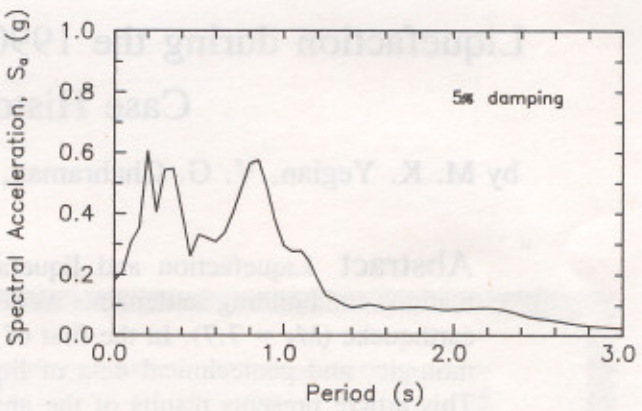

Figure 4. Acceleration response spectrum of the Lahijan record shown in Figure 2.

of magnitude $M_S = 7.7$ is consistent with those obtained from other similar magnitude earthquakes (Seed *et al.*, 1983).

Figure 4 shows the acceleration response spectrum of the Lahijan record. Of particular interest is the spectral peak at about 0.8 sec. This period is most likely associated with the period of the soil profile in Lahijan (at the recording site). To demonstrate this, the period of the soil profile, T_p, is estimated from the relationship $T_p = 4H/V_s$, which is based on the assumption of a simple shear beam model and a uniform soil deposit. Considering a profile thickness, H, of 50 to 70 m and a typical shear-wave velocity, V_s, of 250 m/sec for the alluvium, for a range of densities encountered, the period for the soil profile in Lahijan, T_p, is estimated to be about 0.8 to 1.1 sec—consistent with that observed from the response spectrum. Thus, the ground motions in Lahijan include the potential soil amplification effects. For the reasons given earlier, using the Lahijan record in the analyses of the liquefaction case histories in the Astaneh-Ashrafieh region may consider the potential soil amplification effects.

Liquefaction of Level Ground

Liquefaction from the Manjil earthquake was observed at distances ranging between 15 and 85 km from the ruptured fault. Based on worldwide case histories of liquefaction, it has been demonstrated that during an earthquake of a certain magnitude there is a maximum distance beyond which liquefaction is not likely to occur. Figure 5 shows one such relationship between moment magnitude, M_w, and the maximum distance from a fault, R_f, proposed by Ambraseys (1988). Included in this plot is the range of the data from the 1990 Manjil earthquake. It is of interest to note that during this earthquake, although the maximum distance where liquefaction was observed agrees well with that given by Am-

braseys (1988), it is possible that this distance was limited by the presence of the Caspian Sea. Therefore, liquefaction beyond this proposed maximum distance cannot be precluded, especially if the sands encountered are very loose (Yegian and Vitelli, 1981).

During the authors' survey in the liquefied regions, a number of field observations were made that are of particular interest. For example, in many towns and villages, the water wells were filled with liquefied sands to the same elevation as that of the adjacent ground surface. A typical sand-filled well is illustrated in Figure 6a, while a photograph of such a well is shown in Figure 9 of the companion article (Yegian *et al.*, 1995). This observation of water wells filled with liquefied sand to the elevation of the ground surface provides the field evidence that at the time of liquefaction for the level ground condition, the pore pressure ratio, $r_u = \Delta u/\bar{\sigma}_{v_0}$, at points A and B was equal to 1 (Δu is the excess pore pressure and $\bar{\sigma}_{v_0}$ is the effective vertical stress).

Also in Leef-Shagerd, local residents reported observing water ejecting from the ground to a height (H_w) of about 8 m. A typical sketch of this observation is shown in Figure 6b. From this observation, the depth of liquefaction, d_l, in this region can be estimated. The excess pore water pressure at point C, Δu_C, can be expressed in terms of the height of water above ground, H_w, depth of water table, d_w, and unit weight of water, γ_w, as follows:

$$\Delta u_C = (H_w + d_w)\gamma_w. \quad (1)$$

Considering that at the time of liquefaction $r_u = 1.0$,

$$\Delta u_C = \bar{\sigma}_{v_0} = d_w\gamma_T + (d_l - d_w)\gamma_b \quad (2)$$

$$(H_w + d_w)\gamma_w = d_w\gamma_w + d_l\gamma_b, \quad (3)$$

where the right-hand side is the expression for initial vertical effective stress at point C and γ_b is the buoyant unit weight of the soil. Solving for d_l from equation (3) leads to

$$d_l = H_w(\gamma_w/\gamma_b). \quad (4)$$

Thus, in Leef-Shagerd, where H_w was reported to be about 8 m, assuming a soil unit weight of 1.8 t/m^3, the maximum depth to the liquefaction is estimated to be about 8.0(1.0/0.8) ≈ 10 m. This is consistent with the soil profile in Leef-Shagerd determined by geotechnical field investigations, which indicates the presence of a sand layer extending down to a depth of 10 m. The borehole logs for Leef-Shagerd also show a second sand layer between the depths of 15 and 24 m (Fig. 19 of the companion article), which has a density similar to the shallower layer. The analysis in Leef-Shagerd indicates that this second and deeper layer most likely did not liquefy; otherwise, the height of the water geyser would have been much greater than 8 m.

The above analysis and discussions indicate that field observations and various types of evidence of liquefaction can provide practical information in the investigation of an earthquake-induced liquefaction.

To evaluate the liquefaction strength of the sands encountered in northern Iran, the SPT results from nine towns and 31 boreholes were analyzed (two borehole logs in Roudboneh, showing mostly clay, were excluded). Table 1 summarizes the relevant data from these case histories. The peak ground accelerations were estimated based on the recorded ground-motion data and the attenuation relationship shown in Figure 1. The earthquake-induced average shear stresses, τ_{av}, within the sand deposits were calculated following the procedure described by Seed *et al.* (1983). The field SPT N-values were corrected for the overburden pressure, again in accordance with Seed *et al.* (1983). The average corrected SPT values, $(N_1)_{60}$, for each borehole, and the percent fines are also included in Table 1. In most of the cases analyzed, liquefied sands had less than 10% fines.

Figure 7 shows a plot of the case history data together with the liquefaction strength curves published by Seed *et al.* (1983) for $M = 7.5$ and 8.5. It is noted that the SPT N-values for the case histories reported were ob-

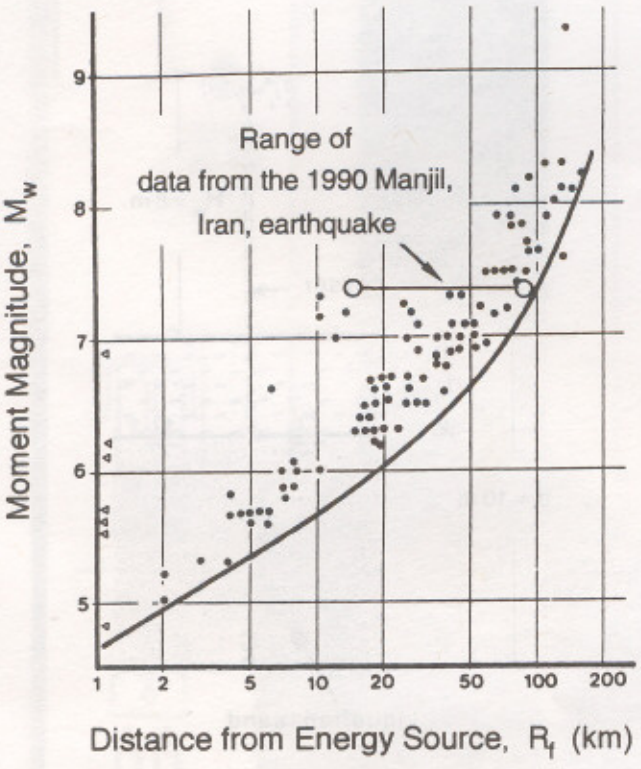

Figure 5. Moment magnitude versus distance from energy release for liquefaction case histories, and the "maximum distance" curve proposed by Ambraseys (1988).

tained after the earthquake. Prior to the earthquake, these values might have been smaller. However, the log from a pre-earthquake borehole near Astaneh-Ashrafieh (AS-Pre-2 in Fig. 12 of the companion article) shows SPT N-values very similar to those recorded after the earthquake in this town. Ohsaki (1966) has made similar observation from the 1964 Niigata earthquake, where he noticed little change in the average SPT N-values of the liquefied sands. Notwithstanding, the liquefaction strength of the sands during the $M_S = 7.7$ Manjil earthquake is in general agreement with the range suggested by Seed *et al.* (1983) for $M = 7.5$ to 8.5, as is illustrated in Figure 7. If one were to make a conservative estimate of the liquefaction strength of these sands for a similar ($M_S = 7.7$) earthquake in the future, the strength values given by Seed *et al.* (1983) for $M = 8.5$ seems to be more appropriate.

Permanent Ground Deformation

There was extensive liquefaction-induced damage in the town of Roudboneh located along the Heshmat river. A typical soil profile in Roudboneh is shown in Figure 8. In this figure, various observations are depicted, including roadway cracks, building settlement by as much as 70 cm, sand boils, and permanent lateral and vertical ground deformations of as much as 100 and 80 cm, respectively. From the results of our field survey and of the geotechnical site investigations, it became evident that liquefaction occurred in the slightly slanting sand deposit shown in Figure 8. Consequently, lateral sliding toward the river was initiated, resulting in permanent ground deformations.

Stability and deformation analyses of the cross section shown in Figure 9 provide back estimates of the residual shear strength of the liquefied sands. During the earthquake, permanent deformations were initiated as the shearing resistance of the sands was reduced by the earthquake-induced excess pore pressures. At the end of the ground shaking, the shearing resistance of the sands, although reduced, must have still been large enough to maintain the static stability of the deformed soil profile. The field survey and subsequent deformation analysis that are described herein indicate that there was no post-earthquake "flow"-type slope failure at this site; otherwise, the deformations would have been much larger than observed. Hence, the static factor of safety at the end of the earthquake shaking must have been greater than 1.0. Therefore, from a static slope stability analysis and assuming a factor of safety F.S. = 1.0, the *minimum* value of the residual shear strength of the liquefied sands can be back calculated.

The results of static stability analyses considering two critical slip surfaces are shown in Figure 9. The soil strength parameters (c and ϕ) used in stability analysis

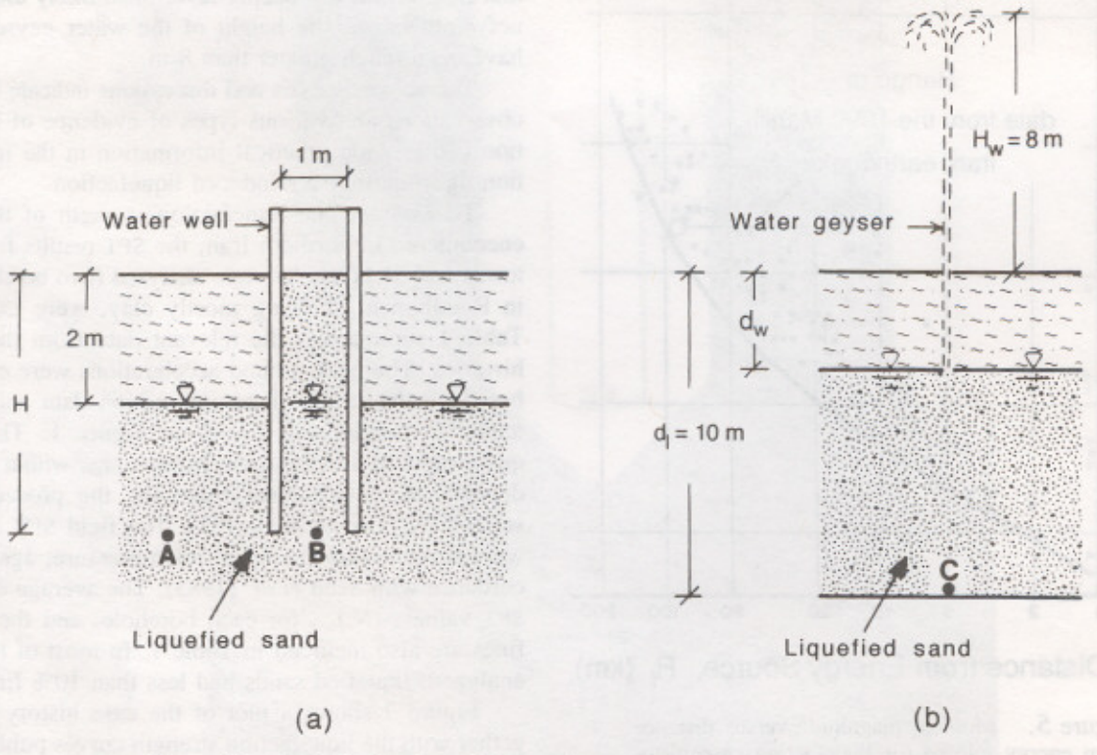

Figure 6. Typical sketches of observations made in the liquefaction region, (a) well filled with liquefied sands; (b) water ejecting from liquefied ground.

for pre-earthquake conditions were estimated from the SPT N-values. The results of these analyses indicate that prior to the earthquake, the slip surfaces were quite stable and factors of safety were larger than 3.0. Also, in Figure 9, the static stability analyses results corresponding to end-of-earthquake conditions are exhibited. In these analyses for each slip surface, a factor of safety of unity was assigned and the residual shear strength of the liquefied sand was back calculated. The results indicate that the *minimum* value of the residual shear strength of the liquefied sands considering slip surfaces 1 and 2 must have been equal to 17.5 and 27.5 kPa, respectively.

Alternatively, an estimate of the *actual* magnitude of the residual shear strength of the liquefied sands can be made from the analysis of permanent ground deformations. In this approach, the residual shear strength of the sands are back estimated by matching the calculated permanent deformations of the slip surfaces with those observed in the field.

The computer program developed by Yee and Yegian (1994) for analysis of permanent deformations was utilized in this investigation. The program calculates the permanent deformation of a single degree of freedom system—representing a mass of soil—relative to a rigid support that is subjected to earthquake excitations. The analytical model incorporates a rigid-plastic force-displacement relationship in which the yield force can vary as a function of time. Such a model can appropriately describe the behavior of a loose sand as its shear resistance decreases because of buildup of excess pore pressure.

Figure 10 illustrates the variable yield acceleration, k_y, used in our analysis of permanent deformations. The vertical axis in this figure defines the yield acceleration at which, if exceeded, the soil mass above the slip surfaces shown in Figure 9 will slide. As shown in Figure 3, the ground shaking, as far as liquefaction is concerned, did not start until $t = 18$ sec (in the record). Therefore, the value of yield acceleration during interval $t = 0$ and $t = 18$ sec, where no excess pore water pressure was generated, was obtained from pseudo-static analysis as described by Makdisi and Seed (1978) and Yegian *et al.* (1991). For example, for slip surface 1, the calculated k_y for the interval between $t = 0$ and $t =$

Table 1
Liquefaction Case History Data from the 1990 Manjil, Iran, Earthquake

Location	Distance from the Fault (km)	Peak Ground Acceleration (g)	Boring Number	% Fines (avg)	$(N_1)_{60}$ (blows/ft)	τ_{av}/σ_v	Liq.
Astaneh-Ashrafieh	65	0.18	AS-1	5	10.4	0.17	yes
			AS-2	3	14.7	0.19	yes
			AS-3	8	13.7	0.17	yes
			AS-4	3	12.6	0.18	yes
			AS-5	1	gravel	—	no
			AS-6	3	10.6	0.19	yes
			AS-7	7	clay	—	no
			AS-8	2	12.9	0.17	no
			AS-9	3	10.6	0.19	yes
			AS-10	4	15.1	0.16	yes
			AS-11	5	14.9	0.17	yes
			AS-12	6	11.2	0.20	yes
			AS-13	6	12.6	0.18	yes
			AS-14	5	17.5	0.18	no
			AS-15	6	27.6	0.17	no
			AS-16	5	13.9	0.18	no
Roudboneh	68	0.15	RB-1	4	8.2	0.13	yes
			RB-2	6	8.8	0.12	yes
			RB-4	4	8.9	0.14	yes
Pahmedan	70	0.15	PA-1	3	12.5	0.14	yes
			PA-2	5	13.4	0.14	yes
Nasser-Kiadeh	75	0.12	NK-1	14	7.1	0.13	yes
Payin-Roudposht	81	0.11	RP-1	6	8.6	0.09	yes
			RP-2	4	11.5	0.10	yes
Safra-Basteh	75	0.12	SB-1	11	14.1	0.17	yes
Leef-Shagerd	55	0.20	LS-1	4	10.9	0.16	yes
			LS-2	8	11.4	0.17	yes
Nassir-Mahalleh	32	0.25	NM-1	2	11.6	0.22	yes
			NM-2	5	10.5	0.20	yes
Bala-Bala	15	0.40	bridge	10	14.8	0.31	yes
Loshan			trestle	10	8.9	0.29	yes

18 sec was about 0.40 g, as shown in Figure 10. Considering the cyclic stress ratio, $\tau_{av}/\bar{\sigma}_v$, and the density of the sands in Roudboneh (see Table 1), analysis of liquefaction indicates that the sands would liquefy in two to four cycles. From Figure 3, it can be concluded that sands in Roudboneh experienced two to four cycles of excitation by about $t = 20$ sec (in the record), thus reducing k_y to a minimum value, $k_{y(min)}$, associated with residual shear strength of the liquefied sands. During the interval $t = 18$ and $t = 20$ sec, as a result of buildup of excess pore pressure, yield acceleration of the soil mass decreased from 0.40 g to $k_{y(min)}$. In our analysis, a linear decrease of k_y was assumed (Fig. 10). Sensitivity analysis has shown that this assumption has little effect on the final conclusions from analysis of permanent deformations.

In our investigations, the residual shear strength, hence the minimum yield acceleration, $k_{y(min)}$, was the unknown parameter that had to be calculated. To determine the value of this residual shear strength, first permanent deformations were calculated as a function of the minimum yield acceleration, $k_{y(min)}$, and the results are exhibited in Figure 11. From this figure and the measured values of the lateral permanent deformations of the slip surfaces 1 and 2 (80 and 100 cm, respectively), the minimum yield accelerations, $k_{y(min)}$, were estimated to be 0.02 g for slip surface 1 and 0.014 g for slip surface 2. Finally, to relate these minimum yield accelerations to the residual shear strength of the liquefied sands, again pseudo-static stability analyses were performed for each of the two slip surfaces. The residual shear strength of the sands were back calculated as a function of the minimum yield acceleration, and the results are plotted in Figure 12. From this figure, considering $k_{y(min)} = 0.02\ g$ and 0.014 g, corresponding to the slip surfaces 1 and 2, the residual shear strength of the sands were estimated to be 21.2 and 28.7 kPa, respectively.

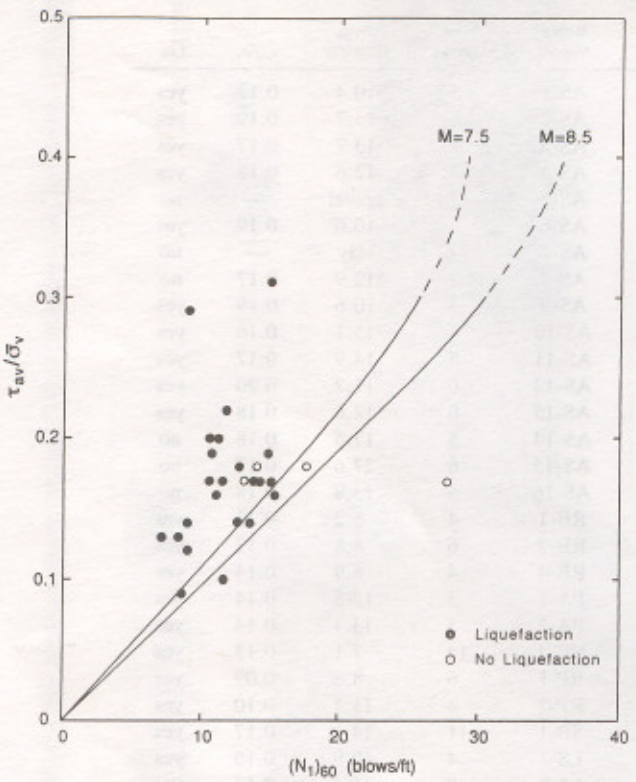

Figure 7. Comparison of the liquefaction case history data from the Manjil, Iran, earthquake (M_S = 7.7) with the liquefaction resistance curves of Seed *et al.* (1983).

As shown in Figure 9, the residual shear strengths calculated from permanent deformation analyses are slightly larger than those estimated from stability analyses. This confirms the earlier statement that the factor of safety at the end of earthquake shaking must have been greater than 1.0 and hence there was no postearthquake slope failure at this site.

Seed *et al.* (1989) have calculated residual shear strength of liquefied sands, as a function of the corrected SPT N values, from many other case histories. In Figure 13, the range of residual shear strength values calculated from our analysis is plotted together with those of Seed *et al.* (1989). It is concluded that the residual shear strength from the Manjil, Iran, earthquake case history is in general agreement with the range suggested by Seed *et al.* (1989) in Figure 13. This case history result from Manjil is also valuable because it plots in the $(N_1)_{60}$ range where data are lacking (Fig. 13).

Liquefaction-Induced Settlement of Buildings

During the Manjil, Iran, earthquake, many buildings, where the foundation sands liquefied, suffered significant damage. Building settlements as large as 100 cm were observed in the liquefaction region. Similar observations have been made from other earthquakes, including 1906 San Francisco (Youd and Hoose, 1978), 1964 Niigata (Ohsaki, 1966), 1965 Alaska (Seed, 1968), and more recently, 1989 Loma Prieta (O'Rourke *et al.*, 1990; Seed *et al.*, 1990), and 1990 Luzon (Adachi *et al.*, 1991) earthquakes. The 1990 Manjil, Iran, earthquake provided the authors with an opportunity to document the geotechnical and building-related data on liquefaction-induced settlement case histories. Analyses of these case histories were performed in order to evaluate the effect of the density of liquefied sands on building settlements. In addition, these settlements are compared with those of level ground observed in Iran, and with values that are predicted by using the procedure of Tokimatsu and Seed (1987). The results of these evaluations follow.

Table 2 lists 10 building settlement case histories and two cases of level ground settlement from the liquefaction region. All of the buildings investigated were one- and two-story brick or masonry block structures with individual or continuous footings. Associated with each

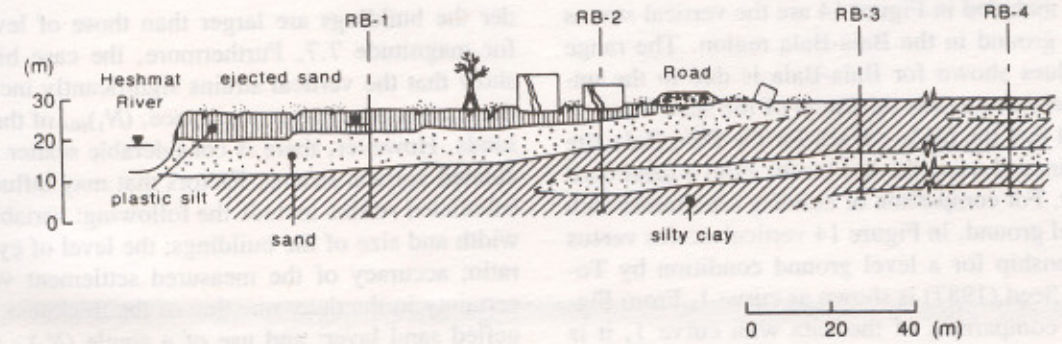

Figure 8. A typical soil profile, and location of boreholes in the town of Roudboneh, with evidence of liquefaction.

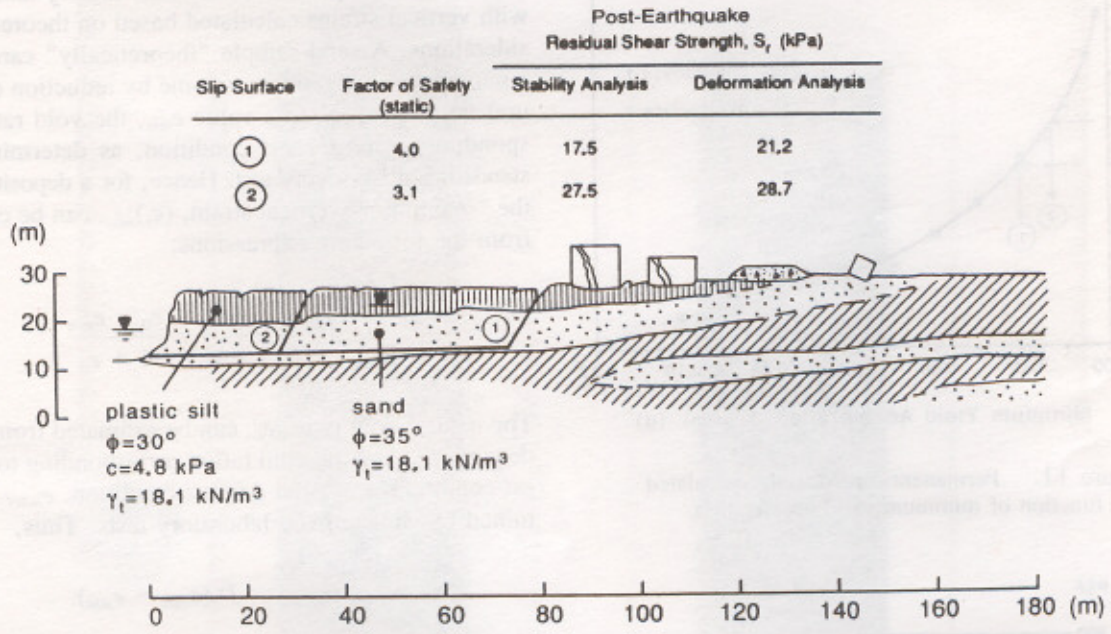

Figure 9. Residual shear strength of liquefied sands, calculated from stability and permanent deformation analyses in Roudboneh.

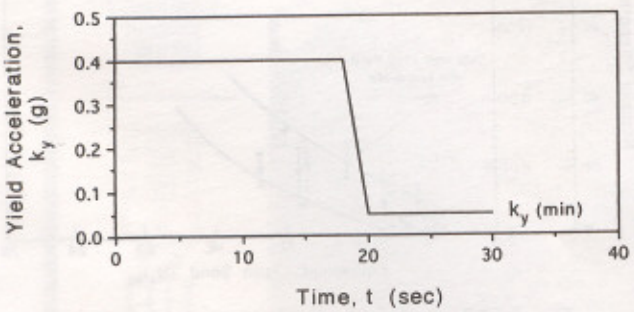

Figure 10. Variable yield acceleration considered in the permanent deformation analyses in Roudboneh.

building is a borehole log (closest to the building) as identified in Table 2, which are described in detail in the companion article. The thickness of the liquefied sands and the average corrected SPT, $(N_1)_{60}$, values for each building site were obtained from the corresponding borehole logs. The maximum settlement of a building was measured relative to the ground surface near the building where liquefaction was not observed. These maximum building settlements, ΔH, were divided by the thickness of the liquefied sand layers, H, to calculate the average vertical strains under the buildings, $\Delta H/H$.

Figure 14 shows a plot of the liquefaction-induced vertical strains as a function of the $(N_1)_{60}$ of the liquefied

sands. Also included in Figure 14 are the vertical strains of the level ground in the Bala-Bala region. The range of strain values shown for Bala-Bala is due to the uncertainty in estimating the thickness of the sand layer. It is also noted that the $(N_1)_{60}$ values for the Bala-Bala site were approximated using the test results from a hand cone penetrometer. For comparison of building settlements with those of level ground, in Figure 14 vertical strains versus $(N_1)_{60}$ relationship for a level ground condition by Tokimatsu and Seed (1987) is shown as curve 1. From Figure 14, and comparison of the data with curve 1, it is evident that the liquefaction-induced vertical strains under the buildings are larger than those of level ground for magnitude 7.7. Furthermore, the case history data show that the vertical strains significantly increase with decreasing penetration resistance, $(N_1)_{60}$, of the liquefied sands. However, there is considerable scatter in the calculated vertical strains. Factors that may influence these calculated strains include the following: variability in the width and size of the buildings; the level of cyclic stress ratio; accuracy of the measured settlement values; uncertainty in the determination of the thickness of the liquefied sand layer; and use of a single $(N_1)_{60}$ value (average) to characterize a building site. Nevertheless, the Manjil earthquake case history data show that the liquefaction-induced vertical strains underneath buildings were two to three times larger than that typically expected from level ground conditions.

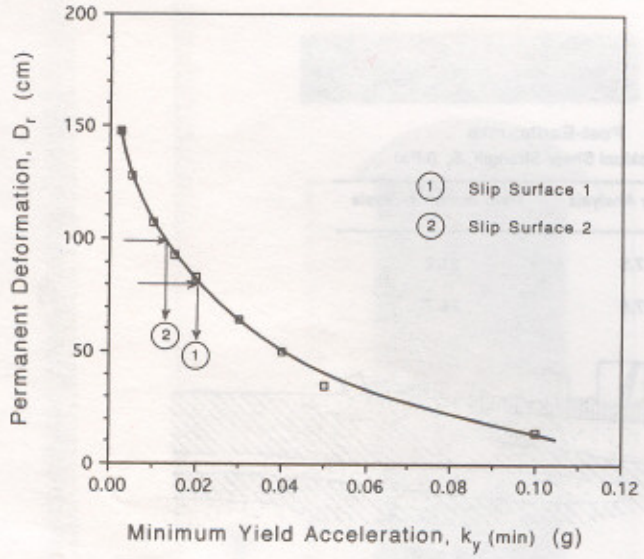

Figure 11. Permanent deformations calculated as a function of minimum yield acceleration.

Further comparison of the case history data is made with vertical strains calculated based on theoretical considerations. A sand sample "theoretically" can undergo a maximum change in its volume by reduction of its natural void ratio, e_0, to a value e_{min}, the void ratio corresponding to its densest condition, as determined by a standardized laboratory test. Hence, for a deposit of sand, the "maximum" vertical strain, $(\epsilon_v)_{max}$, can be calculated from the following expressions:

$$(\epsilon_v)_{max} = \frac{\Delta e}{1 + e_0} = \frac{e_0 - e_{min}}{1 + e_0}. \tag{5}$$

The natural void ratio, e_0, can be estimated from relative density, D_r, and the void ratios corresponding to its loosest condition, e_{max}, and densest condition, e_{min}, as determined by standardized laboratory tests. Thus,

$$e_0 = e_{max} - D_r(e_{max} - e_{min}). \tag{6}$$

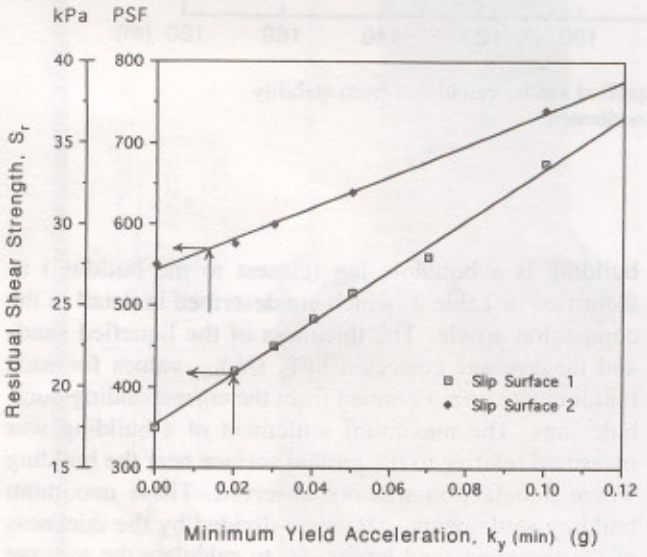

Figure 12. Residual shear strengths estimated based on minimum yield acceleration, for slip surfaces 1 and 2 of Figure 9.

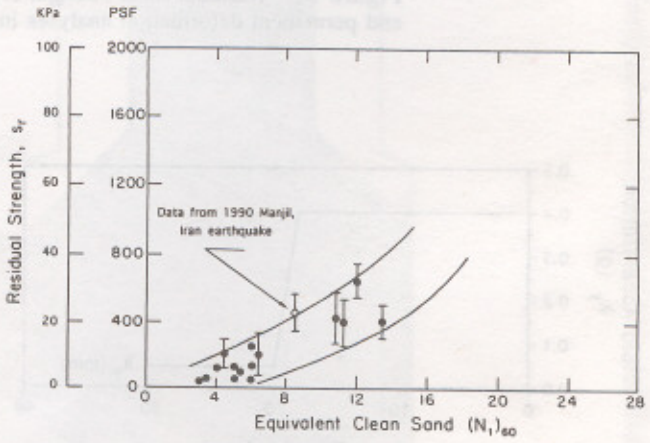

Figure 13. Comparison between values of residual shear strength from Manjil, Iran, case history, and other case histories (after Seed *et al.*, 1989).

Table 2
Case Histories of Liquefaction-Induced Building and Level Ground Settlements from the 1990 Manjil, Iran, Earthquake

Location	Borehole Number	Building Type	Thickness of Sand Layer, H (m)	$(N_1)_{60}$	Maximum Settlement ΔH (cm)	$\Delta H/H$ (%)	% Fines
Astaneh-Ashrafieh	AS-13	one-story unreinforced brick masonry house	12	12.6	20 to 25	1.7 to 2.1	6
	AS-13	two-story unreinforced brick, uniform settlement	12	12.6	50	4.2	6
	AS-13	two-story unreinforced brick masonry house	12	12.6	60	5.0	6
	AS-13	two-story unreinforced masonry house	12	12.6	70	5.8	6
	AS-10	one-story unreinforced brick masonry house	9	15.1	20	2.2	4
Roudboneh	RB-2	one-story brick commercial bldg.	12.5	8.8	60 to 70	4.8 to 5.6	6
Safra-Basteh	SB-1	one-story unreinforced brick school bldg.	5	14.1	15	3.0	11
Payin-Roudposht	RP-1	one-story unreinforced brick school bldg.	10.5	8.6	40	3.8	6
	RP-2	two-story residential unreinforced masonry	17	11.5	100	5.9	4
Nasser-Kiadeh	NK-1	one-story unreinforced masonry police station	4	7.1	30 to 40	7.5 to 10	14
Bala-Bala Region	LO-1	bridge piers (level ground)	8 to 10	14.9*	20 to 30	2.0 to 3.7	10
	LO-3	trestle piles (level ground)	5 to 7	8.6*	20	2.9 to 4.0	10

*Estimated using hand cone penetrometer.

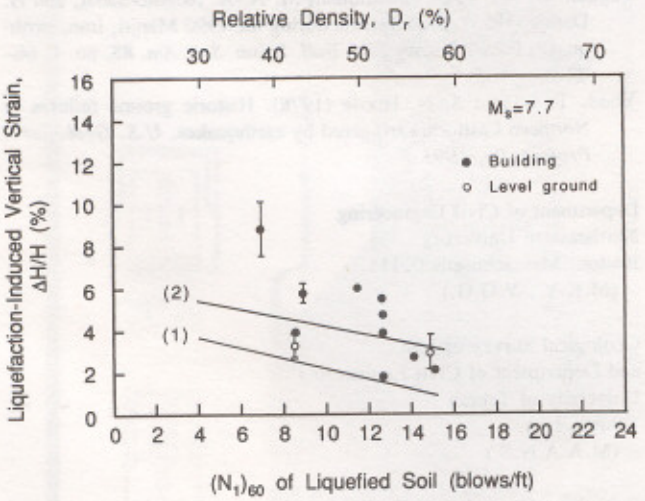

Figure 14. Liquefaction-induced vertical strains as a function of corrected SPT, $(N_1)_{60}$, data from Manjil, Iran, earthquake; curve 1 corresponds to level ground conditions based on Tokimatsu and Seed (1987); and curve 2 corresponds to theoretical maximum vertical strain based on e_{min} and e_{max}.

Curve 2 shown in Figure 14 was generated by calculating maximum vertical strains for a range of D_r using equations (5) and (6), and average values of e_{min} = 1.335 and e_{max} = 1.543 determined from laboratory tests for the sands of the Manjil earthquake case histories. In Figure 14, the relative densities have been related to $(N_1)_{60}$ values by the relationship proposed by Tokimatsu and Seed (1987). A comparison of the case history data with curve 2 indicates that the observed building settlements are generally larger than the "theoretical" maximum settlements calculated using the values of e_{min} and e_{max}. Hence, caution is made in estimating liquefaction-induced settlements solely based on experimental tests where sands are reconstituted to natural void ratios calculated from relative densities and values of e_{min} and e_{max}.

Conclusions

Case histories of liquefaction and liquefaction-induced settlements from the 1990 Manjil, Iran, earth-

quake (M_S = 7.7) were analyzed and the following conclusions were made:

1. Liquefaction was observed as far away as 85 km from the causative fault. This maximum distance agrees well with that given by Ambraseys (1988).
2. Analysis of field observations, such as the level of the liquefied sands in water wells and height of water ejecting out of the liquefied ground, provided pertinent information useful in the determination of the depth of the liquefied sands.
3. The liquefaction strength of the sands during the M_S = 7.7 Manjil earthquake is in general agreement with the range of strength values suggested by Seed *et al.* (1983) for magnitude M = 7.5 to 8.5 earthquakes.
4. Analysis of liquefaction-induced permanent ground deformations indicates that the post-liquefaction residual shear strength of the sands, having an average corrected SPT, $(N_1)_{60}$, value of about 8.5 blows/ft, ranges between 21.2 and 28.7 kPa. This calculated range of residual shear strength is in general agreement with the results published by Seed *et al.* (1989), based on similar case histories from other earthquakes.
5. Analysis of case histories on liquefaction-induced settlement of buildings indicates that the average vertical strains in the liquefied sands underneath the buildings were 2 to 3 times larger than those on level ground.

Acknowledgments

Funding for the field surveys and geotechnical field investigations was provided by the Ministry of Housing and Urban Development of Iran, and the Office of the Governor of the Guilan Province. The authors gratefully acknowledge this support.

References

Adachi, T., S. Iwai, M. Yasui, and Y. Sato (1991). Settlement and inclination of reinforced concrete buildings in Dagupan City due to liquefaction during the 1990 Philippine earthquake, in *Proc. 2nd Int. Conf. on Recent Adv. in Geotech. Earthquake Engineering and Soil Dyn.*, March, St. Louis, Missouri, Vol. **2**, 147–152.

Ambraseys, N. N. (1988). Engineering seismology, *J. Earthquake Eng. Struct. Dyn.* **17**, no. 1, 1–105.

Idriss, I. M. (1990). Response of soft soil sites during earthquakes, *Proc. H. B. Seed Memorial Symposium*, Vol. 2, BiTech Publishers, Vancouver, British Columbia, Canada, 273–289.

Joyner, W. B. and D. M. Boore (1988). Measurement, characterization, and prediction of strong ground motion, in *Proceedings of Earthquake Engineering and Soil Dynamics*, J. L. Van Thun (Editor), ASCE, New York, 43–102.

Makdisi, F. I. and H. B. Seed (1978). Simplified procedure for estimating dam and embankment earthquake-induced deformations, *J. Geotech. Eng.* **104**, no. 7, 849–867.

Nogole-Sadat, M. A. A. (1992). Geologic and seismologic map of Guilan Province, in *Treatise on Geology of Iran*, Geological Survey of Iran, Tehran.

O'Rourke, T. D., H. E. Stewart, F. T. Blackburn, and T. S. Dickerman (1990). Geotechnical and lifeline aspects of the October 17, 1989 Loma Prieta earthquake in San Francisco, Technical Report NCEER-90-0001, January, Buffalo, New York.

Ohsaki, Y. (1966). Niigata earthquake, 1964: building damage and soil conditions, *Soils Foundations* **6**, no. 2, 14–37.

Seed, H. B. (1968). Landslides during earthquakes due to soil liquefaction, *J. Soil Mech. Found. Eng.* **94**, no. 5, 1055–1122.

Seed, H. B., I. M. Idriss, and I. Arango (1983). Evaluation of liquefaction potential using field performance data, *J. Geotech. Eng.* **109**, no. 3, 458–482.

Seed, H. B., I. M. Idriss, F. I. Makdisi, and N. Banerji (1975). Representation of irregular stress time histories by equivalent uniform stress series in liquefaction analysis, Report Number EERC 75-29, University of California, Berkeley.

Seed, H. B., R. B. Seed, L. F. Harder, and H. L. Jong (1989). Re-evaluation of the lower San Fernando dam: examination of the post-earthquake slide of February 9, 1971, Contract Report GL-89-2, Report 2, U.S. Army Corps of Engineers Waterways Exp. Station., Vicksburg, Mississippi.

Seed, R. B., S. E. Dickenson, M. F. Riemer, J. D. Bray, N. Sitar, J. K. Mitchell, I. M. Idriss, R. E. Kayen, A. Icropp, L. F. Harder, Jr., and M. S. Power (1990). Preliminary report on the principal geotechnical aspects of the October 17, 1989 Loma Prieta earthquake, Report Number UCB/EERC-90/05, April, University of California, Berkeley.

Tokimatsu, K. and H. B. Seed (1987). Evaluation of settlements in sands due to earthquake shaking, *J. Geotech. Eng.* **113**, no. 8, 861–878.

Yee, Z. and M. K. Yegian (1994). Evaluation of earthquake-induced permanent deformations of earth dams, Report Number CE-94-10, Department of Civil Engineering, Northeastern University, Boston, Massachusetts.

Yegian, M. K. and B. M. Vitelli (1981). Probabilistic analysis for liquefaction, Report Number CE-81-1, Department of Civil Engineering, Northeastern University, Boston, Massachusetts.

Yegian, M. K., E. A. Marciano, and V. G. Ghahraman (1991). Earthquake-induced permanent deformations: probabilistic approach, *J. Geotech. Eng.* **117**, no. 1, 35–50.

Yegian, M. K., V. G. Ghahraman, M. A. A. Nogole-Sadat, and H. Daraie (1995). Liquefaction during the 1990 Manjil, Iran, earthquake, I: case history data, *Bull. Seism. Soc. Am.* **85**, no. 1, 66–82.

Youd, T. L. and S. N. Hoose (1978). Historic ground failures in Northern California triggered by earthquakes, *U.S. Geol. Surv. Profess. Pap. 993*.

Department of Civil Engineering
Northeastern University
Boston, Massachusetts 02115
(M.K.Y., V.G.G.)

Geological Survey of Iran
and Department of Civil Engineering
University of Tehran
Tehran, Iran
(M.A.A.N.S.)

Consulting Geotechnical Engineer
Tehran, Iran
(H.D.)

Manuscript received 6 January 1994.